Irregular structures observed below 71 km in the night-time polar D-region

E. V. Thrane, T. A. Blix, K. R. Svenes

Ann. Geophysicae 18, 215–222 (2000) © EGS – Springer-Verlag 2000

Annales Geophysicae

Irregular structures observed below 71 km in the night-time polar D-region

E. V. Thrane[1,2], **T. A. Blix**[1], **K. R. Svenes**[1]

[1] Norwegian Defence Research Establishment, P O Box 25, NO-2027 Kjeller, Norway
E-mail: eivind-wilhelm.thrane@ffi.no
[2] Institute of Physics, University in Oslo, P O Box 1048, Blindern, NO-0316 Oslo, Norway

Received: 8 March 1999 / Revised: 13 October 1999 / Accepted: 28 October 1999

Abstract. A new rocket range, SvalRak, was opened in November 1997 at Ny-Ålesund (79°N) in the Svalbard archipelago. The first instrumented rocket was launched on 20 November, 1997, at 1730 UT during geomagnetically quiet conditions. The payload was instrumented to measure plasma parameters in the mesosphere and lower thermosphere, but the payload only reached an altitude of 71 km. This resulted in a very flat trajectory through the lower D-region. The positive ion concentrations were larger than expected, and some unexpected plasma irregularities were observed below 71 km. The irregularities were typically 100 m in spatial extent, with plasma densities a factor of two to five above the ambient background. In the dark polar night the plasma below 71 km must consist mainly of positive and negative ions and the only conceivable ionising radiation is a flux of energetic particles. Furthermore only relativistic electrons have the large energies and the small gyro radii required in order to explain the observed spatial structure. The source of these electrons is uncertain.

Key words: Ionosphere (ionospheric irregularities; ionization mechanisms) – Magnetospheric physics (polar cap phenomena)

1 Introduction

The archipelago of Svalbard is located between latitudes 78° and 81°N, only about 1300 km from the geographic North Pole and 2300 km from the geomagnetic pole. Its position with respect to the auroral zone is unique within the north polar region. During daytime Svalbard lies directly under the cusp region and it is the only landmass from which the daytime aurora can be studied in darkness during the winter months. At night Svalbard lies well within the polar cap. For these reasons Andøya Rocket Range (ARR) has established an ad hoc launch facility for sounding rockets at Ny-Ålesund (78.9°N, 12°E Geographic, 76.1°N, 112.3°E Geomagnetic). The L-shell value is $L = 17$, and the invariant latitude $\Lambda = 78°$. The facility is called SvalRak. The first campaigns from the new range were carried out in November, 1997, and the very first rocket was ISBJØRN 1 launched on 20 November, 1997, at 1730 UT. A second payload, ISBJØRN 2 was successfully launched on a Viper IIIa motor at 2000 UT by the University in Tromsø. This study will describe the ISBJØRN 1 payload with its instruments and present the first scientific results. The ISBJØRN 2 results will be presented elsewhere (O. Havnes University in Tromcø, Norway, private communication).

2 Scientific aims

The mesosphere and lower ionosphere within the polar cap are unexplored in the sense that very few detailed, in-situ measurements have been made. The new launch facility for scientific sounding rockets at Ny-Ålesund therefore offers unique opportunities for pioneer studies. The ISBJØRN 1 payload was designed to measure selected parameters that characterise the state of both the plasma and the neutral atmosphere in the height region 60–120 km. The payload contained two instruments. PIP (positive ion probe) measured positive ion current and CPP (cold plasma probes) measured electron current as well as electron temperature. The latter parameter was to be obtained in the height region above 90 km by means of a sophisticated Langmuir probe technique. Both instruments were designed to obtain accurate, high-resolution data, both on the upleg and downleg of the trajectory. The Langmuir probe measurements are potentially very sensitive to the

Correspondence to: E. V. Thrane

presence of electric fields and geomagnetic disturbances, and therefore geomagnetically quiet conditions were needed during the launch.

Unfortunately, the rocket motor system did not function as specified and the payload only reached an apogee of 71 km. As a consequence the temperature probes did not yield the expected results. The present work will therefore concentrate on the measurements by means of PIP of ion concentration in the lower mesosphere. Positive ions can also be used as passive tracers for variations in the neutral air, and thus, in principle, information about waves and turbulence can be derived (Blix *et al.*, 1990).

3 Experimental method

The payload diameter was 178 mm, the length was 1632 mm and the weight 39.1 kg. It was launched on an Indian Rh300 MkII one-stage motor. The payload was a modified (simplified) version of a TURBO payload flown in earlier campaigns (Blix *et al.*, 1994). It should be pointed out that the TURBO payload type has been very thoroughly tested in 22 successful launches with 17 successful sea recoveries. In fact, the housekeeping section of ISBJØRN 1 was flown for the fifth time.

3.1 The rocket instruments

Figure 1 shows how a central positive ion probe (PIP) and two cold plasma probes (CPP) were mounted under the split nose cone. After nose cone release at about 50 km altitude, the three probes were pushed forward by a spring-controlled telescope, and the two booms carrying the CPPs were deployed sideways. All three probes were thus exposed to the atmosphere outside the shockfront created by the payload.

The Langmuir or cold plasma probes (CPP) collect electron current by sweeping the voltage applied to the outer grid. The two probes had different voltage ranges. The electron temperature and electron densities are in principle derived from the measured voltage-current characteristics. During the ISBJØRN 1 flight the electron current was, unfortunately, below the detection threshold of the instrument.

The positive ion probe (PIP) was centred on the payload axis and is a standard instrument used previously in many payloads (Blix *et al.*, 1990). It is a doubled-grid DC probe, designed to minimise shock front effects by allowing free flow through the probe. The outer grid has a diameter of 12 cm and is at payload potential, whereas the inner grid is biased by −7 V relative to the outer grid. The ion current collected by the inner grid is sampled at 2.441 kHz, providing a spatial resolution of better than 0.5 m when the rocket velocity is taken into account. The resolution is 12 bits with an additional 3 bits for current range indication, yielding an accuracy better than 0.025%.

Fig. 1. The instrument in the ISBJØRN 1 payload. A *central* positive ion probe (PIP) and two cold plasma probes (CPP) were mounted under a split nose cone and released to the atmosphere 60 s after launch

3.2 The ground-based instruments

The geophysical conditions before and during launch were monitored by a number of ground-based instruments which were available on-line in Ny-Ålesund. The list below shows the instruments and the responsible organisations:

1. Magnetometers in Tromsø and at Andenes on the mainland, in Longyearbyen and at Ny-Ålesund. (University in Tromsø and Andøya Rocket Range)
2. The imaging riometer Ny-Ålesund (University of Nagoya)
3. Ionosonde observations in Longyearbyen (the University Studies at Svalbard UNIS, Leicester University)
4. EISCAT Svalbard Radar (ESR)

These instruments provided a good overall picture of the state of the ionosphere and made it possible to monitor the launch conditions. These observations are presented and interpreted by Hall *et al.* (1999).

4 The trajectory

Figure 2 shows the trajectory of the payload launched on the Rh300 Mk II motor. The trajectory was determined by the standard ARR slant range system (Haugen, private communication). This system monitors the Doppler shift of signal from the very stable telemetry transmitter in the payload and provides a trajectory with an accuracy comparable to that of a good tracking radar. The Rh300 Mk II motor was equipped with spin-up motors on the fins to increase the spin rate and stability at launch. As noted earlier, a malfunctioning of the motor system prevented the payload from reaching the nominal apogee. Most likely one or two of the spin-up motors failed. Note that the apogee is only 71 km, and that the point of impact is about 130 km from the launch. The result is that the payload flies nearly horizontally through the lower mesosphere. There was no motor separation, and due to the large drag on the fins the payload axis pointed approximately along the velocity vector during most of the flight. The timer sequence in the payload was set for a nominal apogee of 120 km and the nominal height for nose cone release was 64 km. The reduced performance of the rocket system caused nose cone release at an altitude of 48 km and the PIP measured for 140 s from about 50 km on the upleg, through apogee at 71 km to 48 km on the downleg. The spin rate was 3 Hz and there was a coning of $\pm 15°$ with a period of about 20 s.

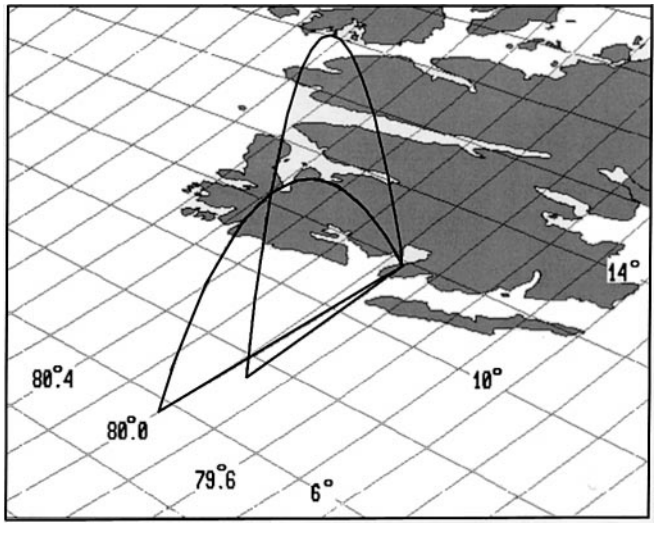

Fig. 2. The nominal (*high apogee*) and the actual (*low apogee*) payload trajectories. The rocket was launched towards the west from Ny-Ålesund (the azimuth angle was 276° from north)

5 Experimental results

5.1 Ground-based observations

The geomagnetic and ionospheric conditions were carefully monitored from the ground for more than a week before the launch of ISBJØRN 1. The monthly averaged sunspot number was 39. Conditions were extremely quiet during this period as well as at the time of launch. The riometers and magnetometers on the mainland and on Svalbard showed no absorption and no significant magnetic activity. Specifically, for the 3-h period containing the launch $K_p = 0_0$. However, sporadic E-layers with critical frequencies of 6–7 MHz were regularly observed during the afternoon periods, and it was decided to launch through such a layer. Below a diffuse and weak F-layer, a partially transparent sporadic E-layer was present just above 100 km with a critical frequency of about 5.5 MHz. The EISCAT radar at Longyearbyen also indicated the presence of ionisation in the E-region. (Hall *et al.*, 1999).

5.2 Satellite observations

To augment the general picture of the geophysical conditions around the time of the ISBJØRN-1 flight some relevant satellite observations are briefly mentioned here. The unusually quiet state of the magnetosphere is readily confirmed by particle measurements from GOES-9 (NOAA, 1999) showing trapped electron flux an order of magnitude smaller at geostationary orbit than in the preceding or the succeeding week. Even so, it should be pointed out that this residual flux still confirms the presence of a significant magnetospheric particle population.

From measurements by the WIND satellite (NASA, 1999) it is also clear that the IMF-B_z was mainly northward for several hours prior to the launch. This, of course, indicates a state of little or no direct coupling between the solar wind and the dayside magnetosphere at that time. In fact it is likely that the magnetosphere may be completely closed for particle entry during such a situation. During such periods the region of closed field lines occupy especially high L-shells. However, it is by no means clear where the dayside field lines couple at the high L-values that are relevant here.

The POLAR satellite (NOAA, 1999) crossed the L-shell of Ny-Ålesund about an hour prior to the launch. This satellite is equipped with several instruments sensitive to particles in the appropriate energy range. However, at that time no high-energy particles were observed. In fact, such particles were not detected until the satellite reached much lower L-values of 8–9 or so. This is in accordance with what is expected from previous trapped particle observations.

5.3 The rocket measurements

In spite of the malfunctioning rocket motor system, the payload behaved nominally during flight and the three

instruments functioned well, both mechanically and electronically. Unfortunately, the low apogee of 71 km prevented the study of the sporadic E-layer, and because the electron density at and below 71 km was below the detection limit, it was not possible to measure electron temperature as planned. The results from the CPP can therefore only provide an upper limit for the electron concentration. In the height region 50–70 km, this upper limit was 10^8 m^{-3}. On the other hand, the positive ion probe provided good results throughout the flight. The ion current measured during the flight from 50 to 220 s is shown in Fig. 3. The apogee at 71 km was reached at 130.5 s. The very low apogee provided an unexpected bonus: it was possible to study horizontal structure in the D-region plasma. Near apogee the payload travelled 17 km in the horizontal direction while the height only changed by 1 km. It is a surprising fact that the current is very variable. Strong current "spikes" are superimposed on a weaker and slowly varying background. The spikes increase in amplitude from the start of the measurements to about five seconds past apogee where they disappear within a few seconds. This indicates that the probe passed through a region where the ion density was patchy and locally enhanced by factors from two to five relative to the background, but that this region was limited in space.

5.4 Possible instrumental causes of the observed enhancements of ion current

The large current spikes have not previously been observed and their source is unknown. The first obvious question is whether the spikes are real increases in ambient plasma density or some artefact generated by the payload and/or instruments. The following points are relevant to this question:

1. The telemetry system functioned well and provided good signal strength with very few dropouts. The SvalSat telemetry station provided an independent telemetry back-up system and the data from the two systems yield the same results.
2. Because of the abnormal trajectory, the instruments were exposed to the atmosphere at a height of 50 km, instead of at the nominal value of 64 km. This must have caused additional drag forces, but there was no indication of any malfunctioning of the payload systems or instruments after nose cone separation.
3. The state and orientation of the payload was monitored with temperature sensors, accelerometers and magnetometers and were found to be as expected. The spin frequency was about 3 Hz and the coning was a moderate ±15° relative to the velocity vector along the trajectory. The observed ion current enhancements are not related to the spin or coning of the payload. In fact no spin or coning modulation was detected in the ion current measured by PIP.
4. There were no high voltages in the electronic systems that could cause corona or other electrical discharges.
5. Fluxes of energetic particles hitting the payload surface will most likely drive the payload potential positive by the release of secondary electrons. Such a mechanism will screen the collector and cause a decrease, not an increase, of positive ion current to the collector.
6. The observed enhancements in ion current typically lasted for 0.2 s, which means that each is described by about 500 samples. Figure 4 shows an example of the observed current for a selected time period.

From these facts we conclude that the irregular enhancements in observed ion current are not of instrumental origin and thus reflect real enhancements of plasma density in the ambient medium.

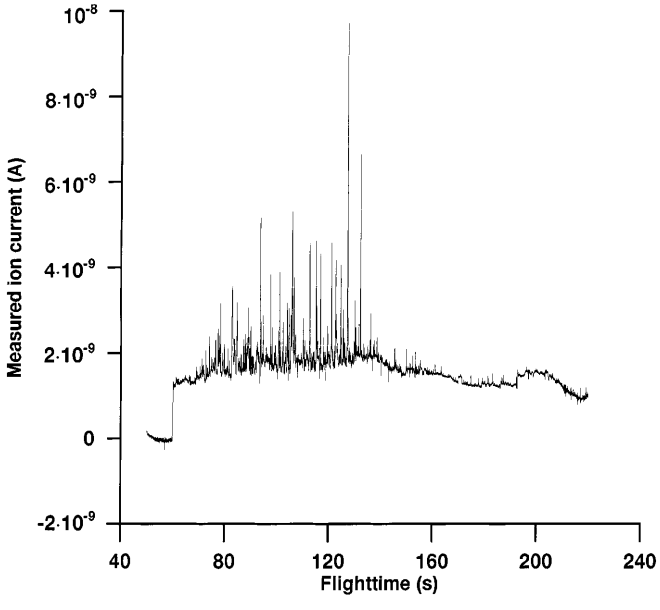

Fig. 3. The ion current observed by PIP during the flight from 50 to 220 s. The apogee was reached at 130.5 s

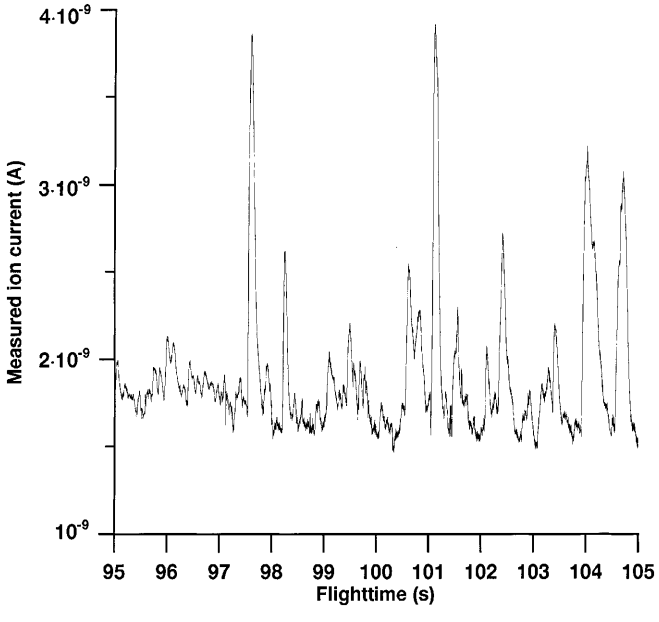

Fig. 4. An example of the detailed structure of the current enhancements in a selected time of flight period

5.5 The observed properties of the ion density enhancements

The concentration of positive ions $N_+(t)$ as a function of flight time t may be derived from the measurements of current $I(t)$ by the simple expression (Blix *et al.*, 1990):

$$N_+(t) = I(t)/\{e\sigma v_r(t)\}$$

where e is the elementary charge, v_r is the rocket speed and σ is the effective cross section of the probe. The rocket trajectory is known so that if we can determine σ, we also know the concentration N_+ as a function of height z, horizontal distance x or the distance s measured along the trajectory. From our past experience we know that the geometric cross section $\sigma_g = 78.5$ cm^2 of the outer grid of the PIP is a good approximation to σ when the payload is not illuminated by solar UV (Blix *et al.*, 1990). The ion current shown in Figs. 3 and 4 are therefore directly proportional to ion density.

It seems clear from Figs. 3 and 4 that the observed ion current is characterised by a slowly varying background of ion density with superimposed distinct peaks that have densities a factor of two to five above the background. We focus attention on the peaks and define a peak as an increase in ion density by a factor of two or more above the background. We describe the properties of the peaks by three parameters: maximum ion density N_{+pm}, the spatial extent δ_s along the rocket trajectory, and the distance λ_s along the trajectory between adjacent peaks. Here δ_s is defined as the width of a peak where the amplitude is $N_{+p} = N_{+pm}/2$, whereas λ_s is the distance between the points of maximum amplitude.

Figure 5 shows the distribution of background and peak amplitude N_{+pm} with height and demonstrates that the peak amplitudes increase with increasing altitude. In Fig. 6 we show the distribution of the spatial extent δ_s of all the 64 peaks we have identified. We note that the mean is $\delta_{sm} = 154$ m and the modal value is about 110 m. Figure 7 shows the distribution of the distance λ_s between the peaks and shows a wide range of values. The mean value, however, is close to 600 m and demonstrates that the peaks are separate and not part of a general noisy background of ion density.

6 Possible physical causes of the observed structures

The observed small-scale ion density enhancements in the dark polar night do not have the characteristics of waves or turbulence in the neutral air or plasma instabilities (Blix *et al.*, 1990, 1994). The enhancements are too large to be explained by any dynamic process redistributing the weak background plasma, for example by adiabatic compression of air particles. We must therefore conclude that an ionising source is present with sufficient energy to penetrate to heights of about 50 km. The most likely candidates are localised beams of precipitating relativistic electrons or protons. At heights below 71 km in darkness the continuity equation for positive ions may be written:

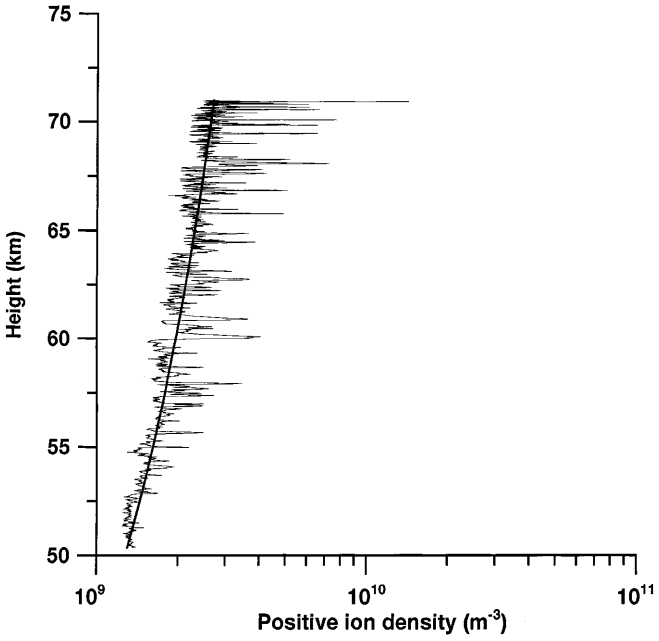

Fig. 5. The background positive ion density N_+ and the peak densities N_{+pm} as a function of height. The *solid line* is an indication, drawn by eye, of the average background ion density

$$\frac{dN_+}{dt} = q - \alpha_i N_+^2 \quad (1)$$

where q is the ion production and α_i is the ion-ion recombination coefficient. We have assumed that electron attachment is dominating so that the concentration of free electrons is very small compared to the concentration of negative ions (Torkar and Friedrich, 1983). In the literature (Conley, 1974) the value of the ion-ion recombination coefficient is quoted to be $\alpha_i = 10^{-13}$ m^3 s^{-1}. Assuming steady state conditions $q = \alpha_i N_+^2$, and Fig. 8 shows the derived ion production rate $q(h)$ for a slowly varying average background

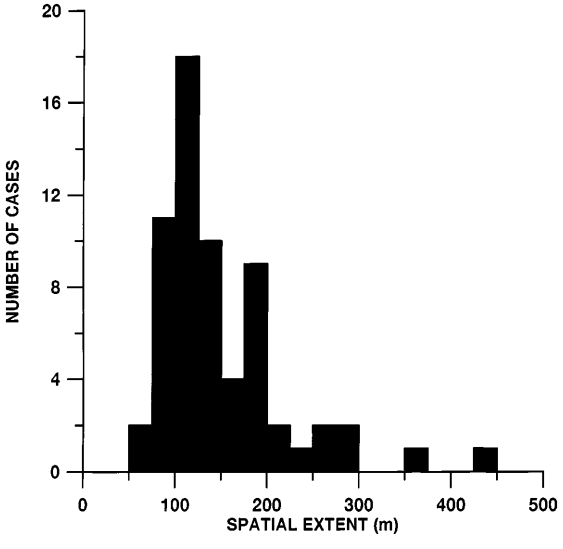

Fig. 6. The distribution of the spatial extent δ_{sm} of the 64 observed peaks

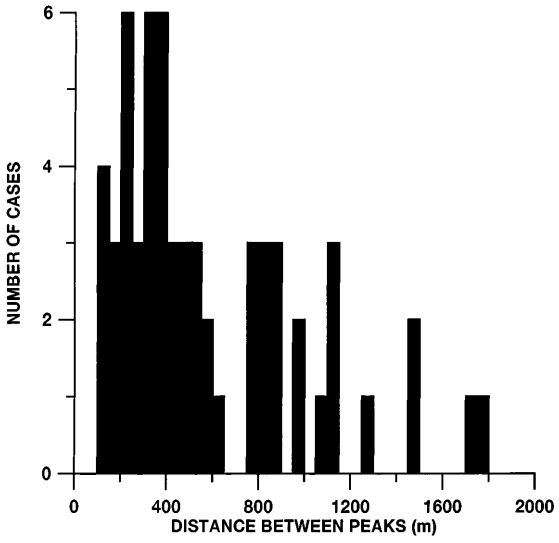

Fig. 7. The distribution of the distance λ_s between adjacent peaks

$N_{+b}(h)$ and for the peaks of the enhancements N_{+pm}. For comparison we also plot the ion production rates expected from cosmic rays for 70°N for solar maximum and minimum conditions (Webber, 1962). We note that near 50 km there is good agreement between our results and the ion production from cosmic rays. The background production varies from $q = 2 \cdot 10^5\ \mathrm{m^{-3}\,s^{-1}}$ at 50 km to $q = 2 \cdot 10^6\ \mathrm{m^{-3}\,s^{-1}}$ at 70 km. The peak production rates are factors of five to twenty above the background, increasing with height.

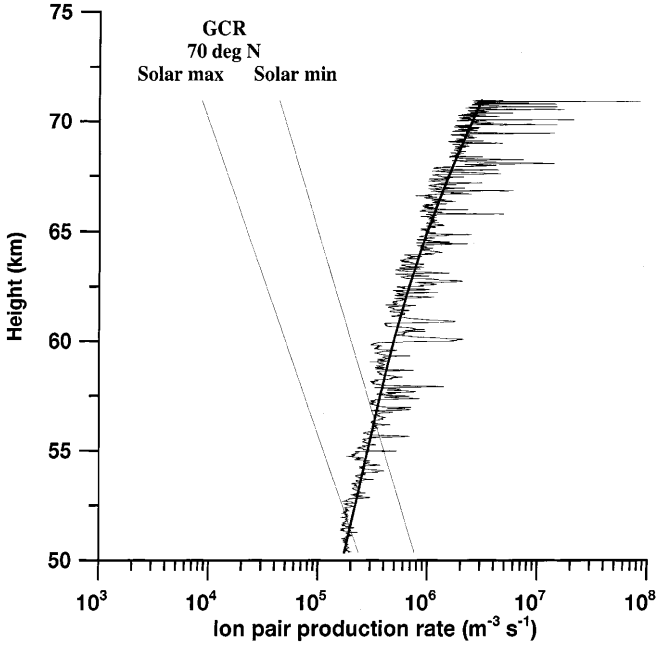

Fig. 8. The derived ion production rate q (h) for the slowly varying background and the peaks. The figure also shows the ion production rate expected from galactic cosmic rays (GCR) at 70°N and for *solar maximum* and *minimum conditions* (Webber, 1962)

6.1 Ionising sources

We note that at 70 km, the background ionisation rate is about 300 times larger than the cosmic ray production. At the time of the ISBJØRN 1 launch the solar zenith angle was 108°, and the only possible electromagnetic ionising radiation that could reach the lower D-region would be Lyman-α scattered from the geocorona. Such radiation can ionise nitric oxide (NO). The flux of Lyman-α has been estimated to be $8.7 \cdot 10^{-7}\ \mu\mathrm{Wm^{-2}}$ at 70 km (see Torkar and Friedrich, 1983 and references therein). Assuming a mixing ratio of NO of 10^{-8} (Brasseur and Solomon, 1984), the ion production at 70 km will be about $500\ \mathrm{m^{-3}\,s^{-1}}$, or more than three orders of magnitude smaller than the ion production by cosmic rays. The most likely sources for the enhanced ion production rates are therefore electrons with energies 200–500 keV or protons with energies 2–20 MeV precipitating along the (almost vertical) magnetic field lines (Berger *et al.*, 1974; Mæhlum, 1973). There is no way in which we can distinguish between electron and proton precipitation as far as the background ion production is concerned. However, if we imagine that concentrated beams of such particles can produce the observed peaks, we find that the gyro radii of particles with the above energies mirroring between 60 and 70 km are approximately 50 m for electrons and 10 km for protons. Thus beams of protons cannot produce enhancements with a horizontal extent of about 100 m, but beams of relativistic electrons remain a possible source.

6.2 The lifetime of plasma enhancements

The beams of relativistic electrons discussed would initially produce near vertical columns of enhanced plasma density. Our plasma probe flying through such columns along the flat trajectory should, on average, observe larger spatial extents of the irregularities on the upleg than near apogee, because the angle of intersection with a hypothetical column changes from about 45° near 50 km to 90° at 71 km. Such a systematic change is not observed, and we must conclude that stationary columns are not present.

Ion-ion recombination, molecular diffusion and dynamic processes such as winds, waves and turbulent diffusion will limit the lifetime of a column of plasma produced below 71 km. We can estimate the order of magnitude of the relevant time scales as follows:

1. The time scale of ion-ion recombination is $\tau \approx 1/(2\alpha_i N_+)$. Using typical values of N_+ for the background and the peaks respectively, we find at 70 km $\tau_b = 2000$ s and $\tau_{pm} = 700$ s.
2. Molecular diffusion may be modelled as $\tau_m \approx L^2/v$ where L is a typical scale and v is the kinematic viscosity of the air. At 70 km $v = 0.17\ \mathrm{m^2\,s^{-1}}$ (US Standard Atmosphere, 1976). Choosing $L = 100$ m, we find $\tau_m = 6 \cdot 10^4$ s.
3. The time scale of turbulent diffusion can be estimated as $\tau_t \approx L/u$ where L is the scale of a turbulent

eddy and u is a typical turbulent velocity. Choosing $L = 100$ m and $u = 1$ ms^{-1}, we find $\tau_t \approx 100$ s.

From these, admittedly very rough, estimates we conclude that the lifetimes of the enhanced plasma densities against recombination and molecular diffusion are very long. The most efficient destruction of a peak will be turbulent diffusion. Unfortunately our measurements of ion density do not permit the derivation of turbulent parameters as described by Blix *et al.* (1990). This is because the background values of N_+ are small and because the peaks will be a dominating influence in a spectral analysis of the measurements, so that turbulence parameters cannot be extracted. We know from experience, however, that turbulence in the mesosphere is patchy, so that there exist limited regions of turbulence interspersed by non-turbulent regions. We therefore propose the following scenario to explain our observations: Very concentrated beams of relativistic electrons produce columns of ionisation in the lower mesosphere. These columns will be broken up and distorted by winds and waves, and wherever there is a localised turbulent region, efficient turbulent diffusion will quickly disperse the enhanced ion density. Outside the turbulent regions, however, the blobs of enhanced ion density may live for thousands of seconds, with sizes corresponding roughly to the cross section of the initial column of ionisation. The rocket payload flies through these blobs and thus maps out a region of electron precipitation that cannot be observed from the ground. This region is also limited in space since ion density peaks are observed only during the first 135 s of the flight.

The intensity of the particle precipitation can be estimated from the derived ion production rates, using the fact that an energetic electron loses an average energy of 35 eV per produced ion pair (Dalgarno, 1962). An electron with an energy of 200 keV will therefore produce about 5700 ion pairs in a column of vertical extent of approximately 10 km and a radius of 50 m. A single electron will thus produce an ion density of about $7.3 \cdot 10^{-5}$ m^{-3}. A typical observed peak density is $5 \cdot 10^{9}$ m^{-3}, requiring about $7 \cdot 10^{13}$ precipitating electrons. These electrons must arrive in a burst, within a period of about 10 s; otherwise the dynamic dispersion processes will not allow the ionisation to build up. Assuming therefore that the precipitation occurs within a column cross section of radius 50 m within 10 s, we arrive at a precipitation intensity of $8.7 \cdot 10^{8}$ electrons m^{-2} s^{-1}.

6.3 Possible origins of the energetic particles

We have no firm evidence to support any specific hypothesis for the origin of localised bursts of relativistic electrons. Nevertheless we should like to discuss briefly some possible mechanisms.

Although we cannot exclude that proton precipitation is responsible for the observed background ionisation, we have no indications from other sources that a weak proton event occurred. On the other hand, it is well known that source populations of electrons in a suitable energy range for inducing electron precipitation exist within the magnetosphere. However, it is also necessary to explain the presence of such high energy precipitation at the very high L-values where these observations very obtained.

One possible source of high energy electrons is a reconnection process occurring in the magnetotail. This hypothesis is supported by the fact that local geomagnetic field lines from Ny-Ålesund map well out into the tail region. According to Nishida and Ogino (1998) reconnection processes are prevalent in the tail even during periods of a weak northward IMF-B_z, as was the case here. The prevailing solar wind conditions at the time was measured by the Wind satellite. For this period the IMF-B_z was about $+2$ nT, while the solar wind density and bulk velocity was on the average 6.5 cm^{-3} and 350 km s^{-1} respectively. By inserting these conditions into the T96-model (Tsyganenko and Stern, 1996), it can be shown that the field line with its foot point at Ny-Ålesund crosses the Geocentric Solar Magnetospheric (GSM) xy-plane at about 30 R_E on the nightside during the relevant time period. Hence, a connection probably existed between the location of our measurements and a region of particle acceleration. It is well known that reconnection regions act as particle accelerators due to the large electric fields produced there. However, in order to produce the filamentary ionisation structures observed from ISBJØRN-1, it is also necessary to assume that the reconnection region was very confined in space and either moving or varying in the time domain. At the present time reconnection processes are not sufficiently well understood to allow a quantitative comparison with our observations.

Several possible, but less likely processes have been considered:

1. *Unstably trapped particles*. In a classical paper Kennel and Petscheck (1966) outlined a process whereby stably trapped electrons would diffuse into the loss cone due to the influence of whistler mode noise. However, two other prerequisites would also have to be fulfilled. First, some inhomogeneity must be present in the source region either in the form of a non-uniform wave field or particle source in order to explain the spatial distribution of our observations. In addition, some process must have lead to these energetic electrons pre-existing at such high L-shells.

2. *Energetic particles in the cusp*. Chen *et al.* (1997) first described this type of population. Their initial observations were based on the measurements of multiply charged ions at high energies in the outer cusp (7–9 R_E) region. Most of these observations occurred in the post-noon sector and were encountered all the way between 50° and 80° latitude as reported by Chen *et al.* (1998). These authors even suggested that the outer cusp region might be viewed as a major new magnetospheric acceleration region. However our launch occurred well into the evening sector, and it is therefore not very likely that such particles should be present.

3. *Sprites*. For completeness it should also be mentioned that narrow columns of ionisation could be

created by electrons accelerated in electrical discharge processes above thunderclouds. These are associated with the optical phenomena known as sprites. In particular, Wescott *et al.* (1998) has reported "columniform" sprites exhibiting mainly vertical structures with very narrow horizontal features (<490 m, their pixel resolution). If such features are the results of accelerated electrons, as is widely believed, they would leave traces similar to those observed from the ISBJØRN-1 rocket. The meteorological office in Tromsø reported that a cold front with unstable air passed Svalbard three days prior to the launch, but that the weather situation was stable during the launch. Hence it is seems unlikely that such a process was active in this case.

7 Conclusion

The ISBJØRN 1 payload was launched in the polar night during very quiet geomagnetic conditions. The instruments observed a plasma background in the height region 50 to 71 km that was consistent with ionisation by galactic cosmic rays near 50 km, but was too dense to be explained by this source above 50 km. The most likely source is therefore precipitating energetic electrons and/or protons. Distinct, strong plasma enhancements were superimposed on the background. The character of these irregularities leads us to believe that they are caused by concentrated beams of relativistic electrons with energies of the order of 200–500 keV. The origin of such precipitation within the nighttime polar cap is not known, but reconnection processes in the magnetotail are possible candidates.

Acknowledgements. Topical Editor F. Vial thanks M. Friedrich and another referee for their help in evaluating this paper.

References

Berger, M. J., S. M. Seltzer, and K. Maeda, Some new results on electron transport in the atmosphere, *J. Atmos. Terr. Phys.*, **36,** 591–671, 1974.

Blix, T. A., E. V. Thrane, and Ø. Andressen, In situ measurements of the fine-scale structure and turbulence in the mesophere and lower thermosphere by means of electrostatic positive ion probes, *J. Geophys. Res.*, **95,** 5533–5548, 1990.

Blix, T. A., E. V. Thrane, S. Kirkwood, and K. Schlegel, Plasma instabilities in the lower E-region observed during the DYANA campaign, *J. Atmos. Terr. Phys.*, **56,** 1853–1870, 1994.

Brasseur, G., and S. Solomon, *Aeronomy of the middle atmosphere*, D. Reidel, Dordrecht, The Netherlands, 1984.

Chen, J., T. A. Fritz, R. B. Sheldon, H. E. Spence, W. N. Spjeldvik, J. F. Fennel, and S. Livi, A new, temporarily confined population in the polar cap during the August 27, 1996 geomagnetic field distortion period, *Geophys. Res. Lett.* **24,** 1447–1450, 1997.

Chen, J., T. A. Fritz, R. B. Sheldon, H. E. Spence, W. N. Spjeldvik, J. F. Fennel, S. Livi, C. T. Russel, J. S. Pickett, and D. A. Gurnett, Cusp energetic particle events: implications for a major acceleration region of the magnetosphere, *J. Geophys. Res.*, **103,** 69–78, 1998.

Conley, T. D., Mesopheric positive ion concentrations, mobilities, and loss rates obtained from rocket-borne Gerdien condenser measurements, *Radio Sci.*, **9,** 575–592, 1974.

Dalgarno, A., *Atomic and molecular processes*, Ed. D. R. Bates, Academic Press, London, 1962.

Hall, C. M., A. P. Van Eyken, and K. R. Svenes, Plasma density over Svalbard during the ISBJØRN campaign, *Ann. Geophysicae*, this issue, 1999.

Kennel, C. F, and H. E. Petschek, Limit on stably trapped particle fluxes, *J. Geophys. Res.*, **71,** 1–28, 1966.

Mæhlum, B. N., *Particles precipitation*: *scattering and absorption,* in *Cosmical geophysics*, Eds. A. Egeland, Ø. Holter and A. Omholt, Universitetsforlaget, Oslo, Norway, 1973.

NASA, http://cdaweb.gsfc.nasa.gov/cdaweb/sp_phys/, 1999.

Nishida, A. and T. Ogino, Convection and reconnection in the Earth's magnetotail, in *New perspectives on the Earth's magnetotail*, Eds. A. Nishida, D. N. Baker, and S. W. H. Cowley, 61–75, 1998.

NOAA, http://julius.ngdc.noaa.gov:8080/production/html/GOES/index.html, 1999.

Torkar, K. M, and M. Friedrich, Tests of an ion-chemical model of the D- and lower E-region, *J. Atmos.Terr. Phys.*, **45,** 369–385, 1983.

Tsyganenko, N. A., and D. P. Stern, Modelling the global magnetic of the large-scale Birkeland current systems, *J. Geophys. Res.*, **101,** 27 187–27 198, 1996.

Webber, W., The production of free electrons in the ionospheric D layer by solar and galactic rays and the resultant absorption of radio waves, *J. Geophys. Res.*, **67,** 5091–5106, 1962.

Wescott, E. M., D. D. Sentman, M. J. Heavner, D. L. Hampton, W. A. Lyons, and T. Nelson, Observation of "columniform" sprites, *J. Atmos. Solar-Terr. Phys.*, **60,** 733–740, 1998.

US Standard Atmosphere, NOAA-S/T 76-1562, US Government Printing Office, Washington, USA, 1976.